

Resonance-assisted drastic transition in single-molecule magnets

Lei Gu(古磊), Jia Luo(罗佳), Ruqian Wu, and Guoping Zhao(赵国平)
Citation: Chin. Phys. B, 2025, 34 (**12**): 127501. DOI: 10.1088/1674-1056/ade858
http://cpb.iphy.ac.cn; http://iopscience.iop.org/cpb

What follows is a list of articles you may be interested in

Magnetic-field-controlled spin valve and spin memory based on single-molecule magnets

Zhengzhong Zhang(张正中), Ruya Guo(郭儒雅), Rui Bo(薄锐), and Hao Liu(刘昊)
Chin. Phys. B, 2023, 32 (**9**): 097502. DOI: 10.1088/1674-1056/accf7c

From microelectronics to spintronics and magnonics

Xiu-Feng Han(韩秀峰), Cai-Hua Wan(万蔡华), Hao Wu(吴昊), Chen-Yang Guo(郭晨阳), Ping Tang(唐萍), Zheng-Ren Yan(严政人), Yao-Wen Xing(邢耀文), Wen-Qing He(何文卿), and Guo-Qiang Yu(于国强)
Chin. Phys. B, 2022, 31 (**11**): 117504. DOI: 10.1088/1674-1056/ac9048

Bias-controlled spin memory and spin injector scheme in the tunneling junction with a single-molecule magnet

Zheng-Zhong Zhang(张正中) and Hao Liu(刘昊)
Chin. Phys. B, 2021, 30 (**6**): 067501. DOI: 10.1088/1674-1056/abd9b1

A new manganese-based single-molecule magnet with a record-high antiferromagnetic phase transition temperature

Cui Yan (崔岩), Li Yan-Rong (李艳荣), Li Rui-Yuan (李瑞元), Wang Yun-Ping (王云平)
Chin. Phys. B, 2014, 23 (**6**): 067504. DOI: 10.1088/1674-1056/23/6/067504

Resonance-assisted drastic transition in single-molecule magnets

Lei Gu(古磊)[1,†], Jia Luo(罗佳)[1], Ruqian Wu[2], and Guoping Zhao(赵国平)[1,3,‡]

[1] *College of Physics and Electronic Engineering, Sichuan Normal University, Chengdu* 610068, *China*
[2] *Department of Physics and Astronomy, University of California, Irvine, California* 92697, *USA*
[3] *Center for Magnetism and Spintronics, Sichuan Normal University, Chengdu* 610068, *China*

(Received 6 May 2025; revised manuscript received 23 June 2025; accepted manuscript online 26 June 2025)

Using exact diagonalization of the Hamiltonian and transition matrix in the energy eigenbasis, we perform model calculations of the magnetic relaxation rate in single-molecule magnets. A careful examination of the transition matrix reveals that resonant tunneling does not enhance transitions between the nearly degenerate states; rather, it suppresses them. Instead, transitions from one state in the degenerate pair to neighboring states of the other are significantly enhanced. We conduct a detailed analysis of the transition rates to clearly demonstrate how resonant tunneling modulates these processes. This work provides a substantial reinterpretation of the resonant magnetic relaxation in single-molecule magnets and clearly identifies the dominant relaxation pathways.

Keywords: single-molecule magnets, resonant tunneling, resonant magnetic relaxation

PACS: 75.50.Xx, 76.30.–v, 76.60.Es

DOI: 10.1088/1674-1056/ade858 **CSTR:** 32038.14.CPB.ade858

1. Introduction

Single-molecule magnets (SMMs) have attracted great interests in recent decades for potential applications in quantum information technologies.[1–5] Being basically paramagnetic, magnetic relaxation is inevitable, and the underlying mechanism is one of the central research topics. Except at temperature close to absolute zero, spin–phonon coupling is a prevailing cause, leading to Orbach, Raman, and direct relaxation processes.[6–16] Hyperfine interaction can result in flip of the electron spin by exchanging angular momentum with nuclear spins.[17–20] In a sweep magnetic field, spin polarization can be reversed stochastically through Landau–Zener tunneling effect.[21–25] These magnetic relaxation processes play a crucial role in the magnetic hysteresis behavior of SMMs, and offer potential means to control the magnetic state.

In varying external magnetic fields, the magnetic relaxation in SMMs generally undergoes one or more resonances, characterized by peaks in the relaxation rate, valleys in the relaxation time, or sharp changes in the magnetic hysteresis loops.[22,26–38] These resonances are attributed to spin tunneling between two nearly degenerate states when the magnetic field induces level-crossing between two spin states,[33,34,39–41] hence named resonant spin tunneling. Landau–Zener tunneling flips the spin only around zero-field, but magnetic relaxation resonances are strong at level-crossing induced by the magnetic field. Furthermore, while both Landau–Zener tunneling and hyperfine interaction tunneling are temperature insensitive, resonant magnetic relaxation exhibits a clear temperature dependence, even below $T = 1$ K.[22] Therefore, spin–phonon coupling relaxation is the major cause, and the direct process as the first order effect should be the primary contributor.[34,39–41]

Most SMMs that exhibit magnetic hysteresis possess strong easy-axis magnetic anisotropy,[42–59] which generates an energy barrier that enables slow magnetic relaxation. Since the transverse anisotropies are typically small, they are perturbative compared to the axial anisotropy. Additionally, the spin–phonon coupling is generally weak. These two properties allow analytical derivation of master equations using the quantum perturbation theory. However, theories formulated in the spin eigenbasis may incur inconsistency due to the application of Fermi's golden rule to transitions between two spin eigenstates. Since the spin eigenstates are not necessarily energy engenstates, the transition energy and energy of the involved phonon can be ambiguous. This in turn implies that the transition in this situation is not well-defined. Therefore, calculations based on energy eigenbasis are most consistent for investigations on phonon-mediated relaxation.[60]

We reexamine the magnetic relaxation process around the resonant tunneling using exact diagonalization of the Hamiltonian and transition matrix in the energy eigenbasis. Our primary contribution is a clarification of the dominant relaxation pathway. Previous theories based on spin eigenbasis suggest that the resonant tunneling induces strong transition between the degenerate spin state. Our calculations in the energy eigenbasis offer a substantially different interpretation of resonant tunneling. We find that resonant tunneling suppresses transi-

†Corresponding author. E-mail: gulei@sicnu.edu.cn
‡Corresponding author. E-mail: zhaogp@uestc.edu.cn

© 2025 Chinese Physical Society and IOP Publishing Ltd. All rights, including for text and data mining, AI training, and similar technologies, are reserved.

tion between nearly degenerate energy eigenstates and induces drastic transitions from these states to their neighboring states. After providing a concise theoretical explanation, we conduct a detailed analysis on the underlying mechanism, focusing on Kramers systems. In the subsections, we demonstrate that a similar mechanism applies to satellite resonances, high field resonances, and resonant magnetic relaxation in non-Kramers systems.

2. Model and methods

We consider an axial spin Hamiltonian that reads

$$\mathcal{H}_{\rm s} = -DS_z^2 - BS_z^4 - g\mu_{\rm b}\mu_0 HS_z. \tag{1}$$

For the Kramers case, we set $S = 9/2$ and the parameters according to Ref. [22]. Namely, $D = 0.608$ meV, $B = 3.0 \times 10^{-3}$ meV, $g = 2$, and the external magnetic field is applied along the z direction throughout this work. The resonant tunneling is induced by a transverse magnetic anisotropy term, for which we use the orthorhombic form $E(S_x^2 - S_y^2)$, and we set $E = 0.001$ meV.

A generic description of spin–phonon coupling for acoustic phonons is the rotational model,[61–63] that is, the lattice dynamics change the direction of anisotropy axes while keeping the molecule rigid. This assumption leads to the Hamiltonian

$$\mathcal{H}_{\rm sp} = \sum_{\alpha=x,y,z}\sum_{\boldsymbol{k}\lambda} \xi^{\alpha}_{\boldsymbol{k}\lambda}\,[\mathcal{H}_{\rm s}, S_\alpha]\,(a^{\dagger}_{\boldsymbol{k}\lambda} + a_{\boldsymbol{k}\lambda}), \tag{2}$$

with

$$\xi^{\alpha}_{\boldsymbol{k}\lambda} = {\rm i}\,{\rm e}^{{\rm i}\boldsymbol{k}\cdot\boldsymbol{r}}(\hat{\boldsymbol{k}} \times \boldsymbol{e}_{\boldsymbol{k}\lambda})\sqrt{\omega_{\boldsymbol{k}\lambda}}, \tag{3}$$

where $\hat{\boldsymbol{k}}$ is the normalized phonon wavevector, and $\boldsymbol{e}_{\boldsymbol{k}\lambda}$ is the polarization unit vector of mode $\boldsymbol{k}\lambda$. Without referring to detailed phonon modes of a specific system, we reduce the coupling to $\xi^{\alpha}_{\boldsymbol{k}\lambda} = \zeta\sqrt{\omega_{\boldsymbol{k}\lambda}}$, where ζ is a scaling factor representing the coupling strength.[63] We set $\zeta = 2 \times 10^{-9}$ s$^{1/2}$, which is close to the value used in Ref. [63] and gives a reasonable time scale.

The transition rate for direct process between two (energy) eigenstates of the spin Hamiltonian ($\mathcal{H}_{\rm s}$) can be obtained by the Fermi's golden rule. For instance, the transition rate from $|n\rangle$ to $|n'\rangle$ is given by

$$\Gamma_n^{n'} = \frac{2\pi}{\hbar} N(\hbar\omega_{n'n})\rho(\omega_{n'n})\left|\langle n'|\mathcal{H}_{\rm sp}|n\rangle\right|^2. \tag{4}$$

Here, $\rho(\omega_{n'n})$ is the phonon density of states with $\hbar\omega_{n'n} = E_{n'} - E_n$ the energy difference, and the generalized the Bose–Einstein function $N(\omega_{n'n})$ takes the form

$$N(\hbar\omega_{n'n}) = \begin{cases} ({\rm e}^{\beta\hbar\omega_{n'n}} - 1)^{-1}, \\ \omega_{n'n} >= 0 ({\rm e}^{\beta\hbar|\omega_{n'n}|} - 1)^{-1} + 1, \\ \omega_{n'n} < 0. \end{cases} \tag{5}$$

According to the Debye model, the phonon density of states (DOS) is given by $\rho(\omega_{n'n}) = 9\omega_{n'n}^2/\omega_{\rm D}^3$. We set the Debye frequency as $\omega_{\rm D} = 2.0$ meV, within the range of typical values for SMMs.[64] The temperature is set to $T = 0.5$ K unless otherwise noted.

With these transition rates in hand, evolution of the concentration (population proportion) of the spin eigenstates is governed by[7]

$$\dot{\rho}_n = \sum_{n'\neq n} \Gamma^n_{n'}\rho_{n'} - \rho_n \sum_{n'\neq n} \Gamma^{n'}_n. \tag{6}$$

The coefficients form a matrix whose eigenvalues are relaxation rates of the corresponding eigenmodes, which are linear combination of the spin eigenstates. One of the eigenvalues is zero, corresponding to the equilibrium state, and the eigenstate is the Bose–Einstein distribution of the spin eigenenergies. The relaxation time is defined as the smallest non-vanishing relaxation rate, since the relaxation process lasts until the slowest mode fades away. The evolution of the off-diagonal elements of the density operator, i.e., the dephasing process, is neglected here, since in the energy eigenbasis their evolution is decoupled with the diagonal elements that describe the magnetic relaxation (see e.g. Refs. [34,60]).

In the following, we will frequently refer to eigenstates of the spin Hamiltonian (spin eigenstates) and those of S_z operator. Because of the transverse anisotropy is perturbative, the spin eigenstates are predominately composed of one of S_z eigenstates, with small contributions from the others. For notational simplicity, we denote the energy eigenstates by $|n(*)\rangle$, and the S_z eigenstates by $|m = *\rangle$. For instance, $|n(S-1)\rangle$ indicates the energy eigenstate that primarily consists of $|m = S-1\rangle$ as its basis. The notation may cause confusion at the resonance point, because the energy eigenstates therein is nearly equal combination of two $|m\rangle$ states. However, we note that the energy eigenstates are dominated by one of $|m\rangle$ states even slight way from the exact resonance. The $|n(*)\rangle$ state notation generally makes sense, and we do not introduce special notation for the resonance point.

3. Resonance-assisted spin tunneling

3.1. Theoretical explanation

Let us focus on the resonant magnetic relaxation at the level-crossing between $|n(-S)\rangle$ and $|n(S-1)\rangle$ [*cf*. Fig. 1(b)]. When their energy difference is much larger than the transverse anisotropy, first-order perturbation theory states that in $|n(-S)\rangle$ the portion of $|m = S-1\rangle$ is $\langle m = S-1|E(S_x^2 - S_y^2)|m = -S\rangle/(E_{S-1} - E_{-S})$. This portion increases as the energy difference is reduced. Around the level-crossing, however, the perturbation theory fails. Alternatively, the degenerate perturbation theory suggests that at the level-crossing, $|n(S-1)\rangle$ and $n(-S)\rangle$ would be approximately equal-weight

combinations of $|m=-S\rangle$ and $|m=S-1\rangle$. Therefore, for weak transverse anisotropy (small E), we can infer that the portion of $|m=S-1\rangle$ in $|n(-S)\rangle$ increases from a tiny value to the order of $O(1)$ as the energy difference is reduced. For systems of large angular momentum, states are mixed by high order perturbations, but the observation still applies, since the formulation are products of overlaps of the similar form.

One the other hand, in the spin–phonon coupling described by Eq. (2), action of $\mathcal{H}_s$ does not change the spin eigenstates. Since S_x and S_y can decrease or increase the S_z polarization by 1, transition between two spin eigenstates is mediated by the matrix elements $\langle m|\mathcal{H}_{sp}|m'\rangle$ with $m-m'=\pm 1$. As the portion of $|m=S-1\rangle$ in $|n(-S)\rangle$ increases by several orders, the transition between $|n(-S)\rangle$ and the ground state $|n(S)\rangle$ is significantly enhanced. In this picture based on transition between energy eigenstates, the resonant tunneling modulates the relaxation by wavefunction modification, instead of inducing drastic transition between two degenerate states. To clearly identify the dominant relaxation pathway, we will systematically compare the transition rates of the transition enhanced by resonant tunneling and that between the degenerate energy eigenstates. We refer the former as resonance-assisted transition (RAT) and the latter as resonant transition (RT).

3.2. Numerical verification

Based on the spin Hamiltonian and spin–phonon coupling in Section 2, we calculated the relaxation rate as a function of the external magnetic field. As shown in Fig. 1(a), there are three resonance peaks, corresponding to the level-crossings marked with black dots on the energy level diagram in the inset. We first examine the resonance at the lowest level-crossing whose spin state configuration is illustrated in Fig 1(b). In contrast to previous theory, the transition rate between the two nearly degenerate states decreases as they approach each other and reaches a minimum at the level-crossing. The diminishing relaxation rate in Fig. 1(c) implies that relaxation pathways involving the RT are highly suppressed. On the other hand, the transition rate between $|n(-S)\rangle$ and $|n(S)\rangle$ increases sharply and peaks at the level-crossing, consistent with the rate of magnetic relaxation. The dominant relaxation channel is the resonance-assisted transition, rather than the resonant transition.

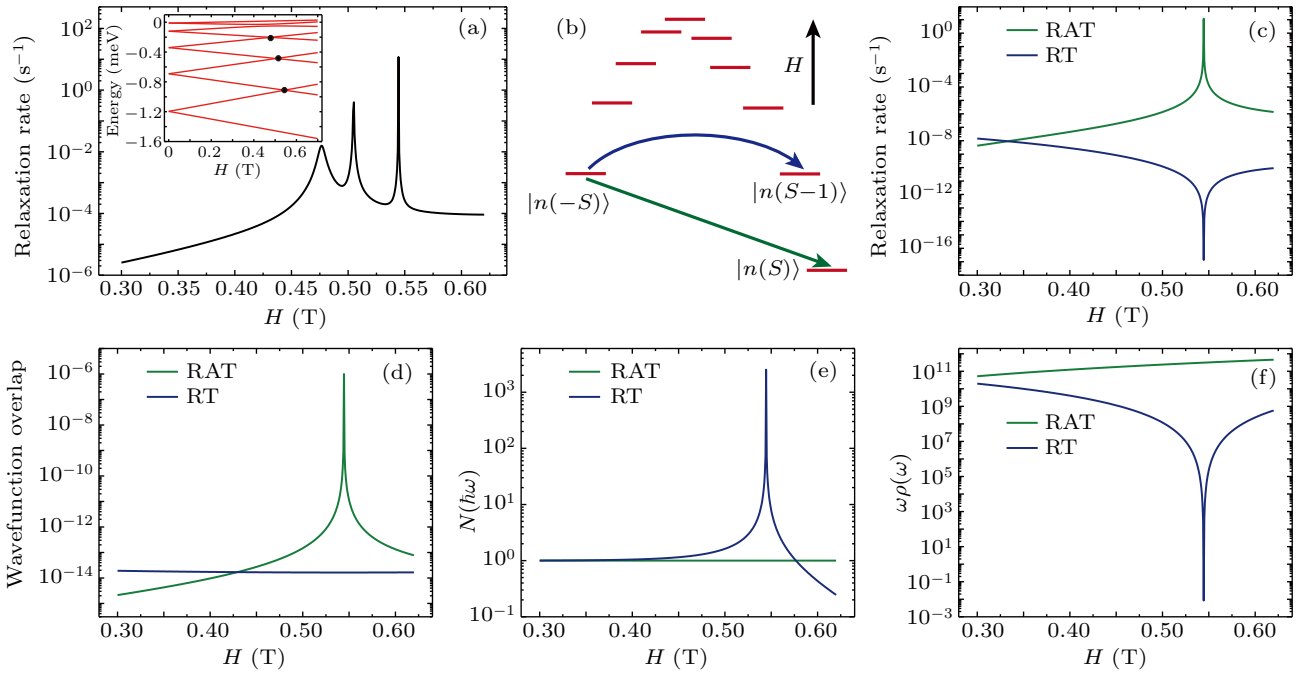


Fig. 1. (a) The relaxation rate for magnetic relaxation resonances at three level crossings. (b) The spin state configuration at the lowest level crossing. (c)–(f) The transition rate, wavefunction overlap, Bose–Einstein function, and the combined scaling factor of the transitions noted in panel (b).

According to Eq. (4), the transition rate consists of three quantities: the inner product, the Bose–Einstein function, and the phonon DOS. In order to highlight the wavefunction overlap by the spin–phonon coupling, we extract the coupling strength $\zeta\sqrt{\omega_{n'n}}$ and recast the transition rate formulation Eq. (4) to

$$\Gamma_n^{n'}=\frac{2\pi\zeta^2}{\hbar}N(\hbar\omega_{n'n})\rho(\omega_{n'n})\omega_{n'n}\left|\langle n'|\mathcal{H}_{sp}/\zeta\sqrt{\omega_{n'n}}|n\rangle\right|^2. \quad (7)$$

Then the last factor represents wavefunction overlap without affected by the coupling strength. We plot the wavefunction overlap, the Bose–Einstein function, and the combined factor $\rho(\omega_{n'n})\omega_{n'n}$ respectively in Figs. 1(d)–1(f) to see how each of these affects the transition rate.

For the resonance-assisted transition, the variation of the DOS factor and Bose–Einstein function are mild compared to the drastic increase of wavefunction overlap. The resonance is primarily driven by the wavefunction overlap, as explained in the previous section. The strong transition relies on the selec-

tion rule $\Delta m = \pm 1$ among the $|m\rangle$ states that is entailed by the rotational spin–phonon coupling. Albeit the rotational model may not provide a complete description, it remains generally relevant, as changing the direction of the anisotropy axis is an almost inevitable consequence of lattice deformation.

The wavefunction overlap between the degenerate states does not have a peak at the level-crossing. Upon examining the wavefunction, we attribute this behavior to a mismatch between the selection rules for the spin–phonon coupling and that for perturbation by the transverse magnetic anisotropy. The term $E(S_x^2 - S_y^2)$ mixes $|m\rangle$ states with $\Delta m = \pm 2$, and the spin–phonon coupling takes effect when $\Delta m = \pm 1$. This means that the effects of this transverse anisotropy and the spin–phonon coupling are orthogonal for half-integer spins. In other words, $|n(-S)\rangle$ are $|n(S-1)\rangle$ are orthogonal in terms of spin-coupling coupling. The transition is made possible by the presence of the magnetic field.

Since the Bose–Einstein function increases approximately exponentially as the energy is lowered to zero, it could potentially lead to a significant enhancement of the resonant transition. However, the combined factor $\rho(\omega_{n'n})\omega_{n'n}$ scale as $\propto \omega_{n'n}^3$, which counteracts or overturns the enhancing effect of the Bose–Einstein function. The factor $\sqrt{\omega_{k\lambda}}$ in the spin–phonon coupling reflects the observation that the lower is the energy of acoustic phonons, the atomic motion is more like translation and the lattice deformation is weaker.[65] Furthermore, the Debye model gives a reasonable description of the phonon DOS for low energy acoustic phonons. Therefore, a scaling factor $\omega_{k\lambda}^3$ in the rate of magnetic relaxation could be a general feature, not limited to the model presented in this work.

3.3. Satellite resonances

To identify the dominant relaxation pathway around the level-crossing between $|n(-S+1)\rangle$ and $|n(S-2)\rangle$ [Fig. 2(a)], in Fig. 2(b) we first examine the transition rates from $|n(-S+1)\rangle$ to $|n(S-2)\rangle$ and from $|n(-S+1)\rangle$ to $|n(S-1)\rangle$. Similar to the lowest level-crossing, the transition between the nearly degenerate states is significantly weakened around the level-crossing, while the transitions from $|n(-S+1)\rangle$ to $|n(S-1)\rangle$ and from $|n(-S)\rangle$ to $|n(S-2)\rangle$ are drastically enhanced. Therefore, the resonance-assisted transition also occurs at level crossing between excited spin states.

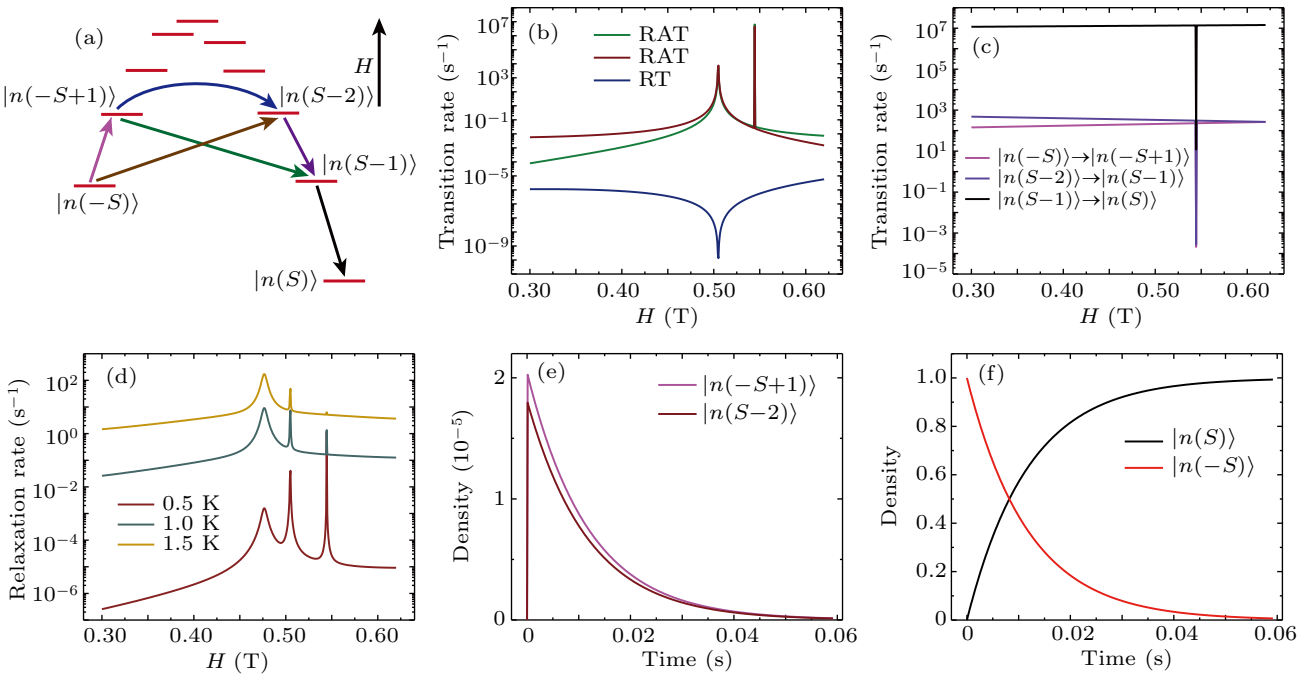


Fig. 2. (a) Spin state configuration for the investigated satellite resonance. (b) and (c) The transition rates of the transitions noted in panel (a). (d) Temperature dependence of the relaxation rates shows that high temperature is favorable to the satellite resonances. (e) The two states in resonance exhibit synchronous evolution. (f) At this low temperature, the density of other states are low, and the relaxation appears to be an overall transition from $|n(-s)\rangle$ to $|n(s)\rangle$.

The magnetic relaxation amounts to an overall transition from $|n(-S)\rangle$ to $|n(S)\rangle$. For the transition from $|n(-S+1)\rangle$ to $|n(S-1)\rangle$ to actually takes effect, the transition from $|n(-S)\rangle$ to $|n(-S+1)\rangle$ and from $|n(S-1)\rangle$ to $|n(S)\rangle$ should be efficient, or otherwise they would function as bottleneck in the relaxation pathway. Because these transitions are well consistent with the selection rule of spin–phonon coupling, the rates should be large. Indeed, as shown in Fig. 2(c), these transition rates are very high. Therefore, around this level-crossing, the magnetic relaxation undergoes the pathway marked by the three straight arrows. The transition from $|n(-S)\rangle$ to $|n(-S+1)\rangle$ (and from $|n(-S+1)\rangle$ to $|n(S-1)\rangle$) involves an energy difference, which weighs the transition rate by the corresponding Bose–Einstein function, so the efficiency of this

pathway is sensitive to temperature variation and should be more efficient at higher temperature. As shown in Fig. 2(d), its absolute and especially relative strength is increased with temperature, in consistent with the observation in Ref. [22].

Besides inducing the drastic transitions, the resonance also manifests as synchronous evolution of the two states in resonance. To show this, the initial state is polarized to $|n(-S)\rangle$, and the magnetic relaxation starts at $t = 0$, at which the magnetic field is instantly set to the strength for inducing the resonance ($H \approx 0.5$ T). As shown in Fig. 2(e), right after starting of the relaxation, the two degenerate states get finite densities (probability of occupation), and then the densities exponentially decay. The identical trends suggest that these two are in resonance. However, because the downward transitions also have high rates, the densities of the intermediate states are low. In terms of the density, the relaxation appears to be a transition from $|n(-s)\rangle$ to $|n(s)\rangle$, as figure 2 shows.

We note that the low occupation probability in Fig. 2(e) does not implies the insignificance of the two states, but rather, these are the dominant intermediate states. The occupation is insignificant because once the system is excited to these states, they quickly decay to the low energy states, although the relaxation is mediated by them. Intuitively, it is like that the system passes these states at a fast pace. Thus, although they are efficient intermediate states, the occupation probability is low at a time. The occupation probability would increase if the temperature is raised.

3.4. Lower symmetry anisotropy and high field resonances

Since state transitions are primarily mediated by key $|m\rangle$ state components in a spin eigenstate, the form of transverse magnetic anisotropy can considerably affect the transition rate. The term $E(S_x^2 - S_y^2)$ considered so far mixed $|m\rangle$ states with $\Delta m = \pm 2$, which favors wavefunction overlap and thus promotes the resonance-assisted transition, while disfavor the resonant transition. In this section, we further add a Stevens operator $F[S^+ + S^-, S_z]_+$ with $F = 0.001$ meV, where S^+ and S^- are the spin ladder operators, and $[\,]_+$ denotes anti-commutation.

Compared to the results in Fig. 1(c), figure 3(a) suggests that the F term weakens the resonance-assisted transition while enhancing the resonant transition. Although the transition rate for the latter still drops sharply around the level-crossing, the wavefunction overlap reaches a peak. The peak implies that the resonant transition also undergoes some resonant enhancement at the level-crossing. However, the overall relaxation rate drop implies that the reduction of phonon DOS and suppression of spin–phonon coupling are strong effects hard to be counteracted.

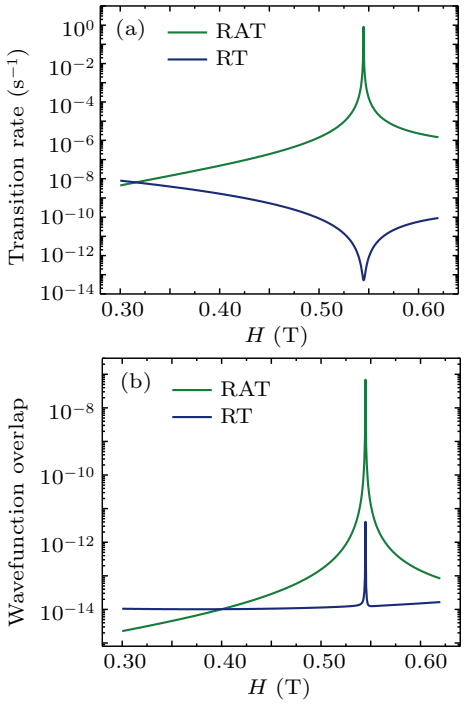


Fig. 3. (a) The F anisotropy term weakens the resonance-assisted transition and strengthens the resonant transition. (b) The wavefunction overlap undergoes a resonance for both types of transition.

When the magnetic field is further increased, level crossing between $|n(-S)\rangle$ and $n(S-2)\rangle$, as well as similar crossings, occurs. We find that in this case, the functional orthogonality between the transverse anisotropy and spin–phonon coupling suppresses the resonant relaxation when only the quadratic transverse anisotropy is present. We neglect this trivial result and calculate the relaxation rate with the inclusion of both the E and F anisotropy terms. As shown in Fig. 4(a), three peaks appear, similar as the results observed at lower field strengths.

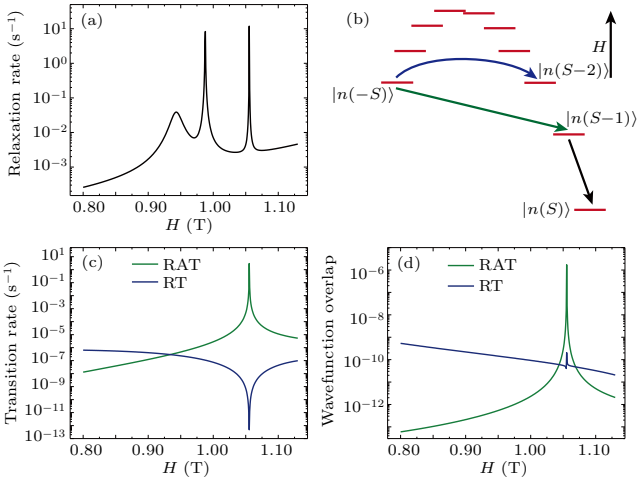


Fig. 4. (a) The relaxation rate suggests that resonant magnetic relaxation occurs at level crossings like that illustrated in panel (b). (c) The transition rate implies that the resonance-assisted transition dominates. (d) Both types of tunneling undergo resonance of wavefunction overlap.

We then inspect the transition rates at the level crossing between $|n(-S)\rangle$ and $n(S-2)\rangle$. Although the wavefunction overlap suggests that the rate of resonant transition peaks

here, the value is still much smaller than that of the resonance-assisted transition. Moreover, the resonant transition is further suppressed by the factor $\propto \omega_{n'n}^3$ which vanishes as $\omega_{n'n}$ approaches zero. The dominant pathway in this case is the one indicated by the straight arrows.

3.5. Non-Kramers systems

In this section, we set the spin to $S = 4$ with all other conditions unchanged. As shown in the relaxation rate in Fig. 5(a), a notable characteristic compared to the Kramers case is the resonance at zero field ($H = 0$ T), which is forbidden by the time-reversal symmetry in Kramers systems. Interestingly, the transition rates suggest that the dominant relaxation pathway is not the direct transition between the two ground states, but instead involves the lowest excited states. At exactly $H = 0$ T, the spin eigenstates are equal-weight superstitions of $|\pm m\rangle$ states. For clarity, in Fig. 5(b) we sketch a spin state configuration under a very weak field, such that the states are polarized. The transition rate in Fig. 5(c) implies that the resonance-assisted transition is much stronger than the resonant transition. The rate difference between the two resonance-assisted transitions lies in the generalized Bose–Einstein function (Eq. (5)), where a downward transition can be much favored compared to a upward transition. For the same reason, the transition from $|n(S-1)\rangle$ to $|n(S)\rangle$ is much stronger than that from $|n(-S)\rangle$ to $|n(-S+1)\rangle$. The two pathways indicated by the straight arrows have comparable efficiency, and they constitute the dominant pathways of the resonant magnetic relaxation.

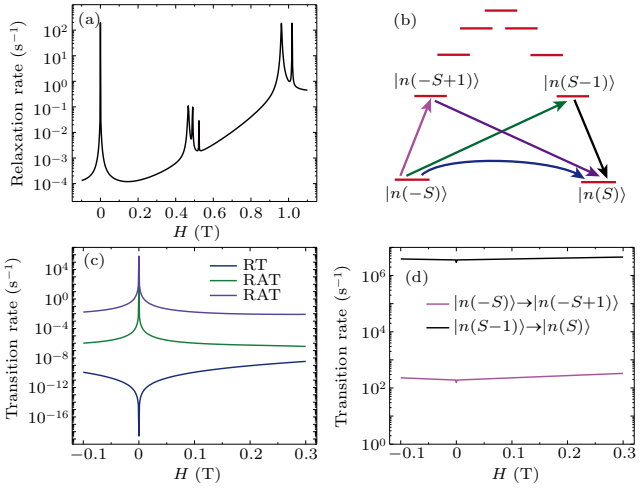


Fig. 5. (a) Non-Kramers systems also have numerous magnetic relaxation resonance, and the one at zero field is notable compared to Kramers systems. (b) The resonance-assisted transitions, marked by the green and purple arrows, apply to the zero-field resonance. (c) and (d) The transition rates implies that the transitions indicated by the straight arrows constitute the dominant pathways for the zero-field resonant magnetic relaxation.

The results here are obtained with both the E and F transverse anisotropy terms included. For the magnetic-field-induced level-crossing similar to those studied in the previous sections, we will not delve into the details. The results are similar: the wavefunction overlap may not have a peak for either tunneling process, depending on the form of the transverse magnetic anisotropy. In general, the resonance-assisted transition is much stronger than the resonant transition, even if the wavefunction overlap of the latter has a resonance, because the factor $\propto \omega_{n'n}^3$ significantly weighs down the rate of the resonant transition.

4. Conclusion

From the perspective of transition among energy eigenstates, the resonant tunneling affects the magnetic relaxation in SMMs through a mechanism distinct from that in theories based on spin eigenstates. Rather than inducing strong transition between the states in resonance, resonant tunneling facilitates resonant magnetic relaxation via wavefuntion modulation, leading to somewhat counter-intuitive relaxation pathways. Although spin–phonon coupling can cause resonant wavefuntion overlap between the nearly degenerate energy eigenstates, the state transition is generally suppressed, due to the suppression of phonon DOS and spin–phonon coupling for low-energy acoustic phonons. On the other hand, the two degenerate states contain substantial mixture of the spin eigenstates at resonance. This state mixture results in strong transitions between the degenerate energy eigenstates and their neighboring states. These drastic transitions facilitate efficient relaxation pathways for the resonant magnetic relaxation.

Acknowledgements

Project supported by the National Natural Science Foundation of China (Grant Nos. 12404085, 12474122, 52171188, 51771127, and 52111530143), the Fund from DOE-BES (Grant No. DE-FG02-05ER46237), and the Central Government Funds of Guiding Local Scientific and Technological Development for Sichuan Province, China (Grant No. 2021ZYD0025).

References

[1] Gaita-Ariño A, Luis F, Hill S and Coronado E 2019 *Nat. Chem.* **11** 301
[2] Coronado E 2020 *Nat. Rev. Mater.* **5** 87
[3] Chilton N F 2022 *Ann. Rev. Mater. Res.* **52** 79
[4] Mirzoyan R, Kazmierczak N P and Hadt R G 2021 *Chemistry - A European Journal* **27** 9482
[5] Kazmierczak N P and Hadt R G 2022 *J. Am. Chem. Soc.* **144** 20804
[6] Shrivastava K N 1983 *Physica Status Solidi (b)* **117** 437
[7] Gatteschi D, Sessoli R and Villain J 2011 *Molecular Nanomagnets* (Oxford: Oxford University Press)
[8] Briganti M, Santanni F, Tesi L, Totti F, Sessoli R and Lunghi A 2021 *J. Am. Chem. Soc.* **143** 13633
[9] Reta D, Kragskow J G C and Chilton N F 2021 *J. Am. Chem. Soc.* **143** 5943
[10] Gu L and Wu R 2020 *Phys. Rev. Lett.* **125** 117203
[11] Gu L and Wu R 2021 *Phys. Rev. B* **103** 014401
[12] Gu L, Li J and Wu R 2022 *J. Magn. Magn. Mater.* **564** 170138

[13] Gu L, Luo J, Luo Q, Zhai Y, Zheng Y Z and Zhao G 2025 *Chin. Phys. Lett.* **42** 027401
[14] Lunghi A 2022 *Sci. Adv.* **8**
[15] Lunghi A 2023 Spin-phonon relaxation in magnetic molecules: Theory, predictions and insights *Challenges and Advances in Computational Chemistry and Physics* (Springer International Publishing) pp. 219–289
[16] Su D, Zhang Y Q, Liu E K and Sun Y 2023 *Chin. Phys. B* **32** 087505
[17] Garanin D A, Chudnovsky E M and Schilling R 2000 *Phys. Rev. B* **61** 12204
[18] Giraud R, Wernsdorfer W, Tkachuk A M, Mailly D and Barbara B 2001 *Phys. Rev. Lett.* **87** 057203
[19] Ishikawa N, Sugita M and Wernsdorfer W 2005 *J. Am. Chem. Soc.* **127** 3650
[20] Chen Y C, Liu J L, Wernsdorfer W, Liu D, Chibotaru L F, Chen X M and Tong M L 2017 *Angewandte Chemie International Edition* **56** 4996
[21] Rousochatzakis I, Ajiro Y, Mitamura H, Kögerler P and Luban M 2005 *Phys. Rev. Lett.* **94** 147204
[22] Wernsdorfer W, Bhaduri S, Vinslava A and Christou G 2005 *Phys. Rev. B* **72** 214429
[23] Vogelsberger M and Garanin D A 2006 *Phys. Rev. B* **73** 092412
[24] Irländer K and Schnack J 2020 *Phys. Rev. B* **102** 054407
[25] Mattioni A, Staab J K, Blackmore W J A, Reta D, Iles-Smith J, Nazir A and Chilton N F 2024 *Nat. Commun.* **15** 485
[26] Thomas L, Lionti F, Ballou R, Gatteschi D, Sessoli R and Barbara B 1996 *Nature* **383** 145
[27] Friedman J R, Sarachik M P, Tejada J and Ziolo R 1996 *Phys. Rev. Lett.* **76** 3830
[28] Hernández J M, Zhang X X, Luis F, Bartolomé J, Tejada J and Ziolo R 1996 *Europhys. Lett.* **35** 301
[29] Barbara B, Thomas L, Lionti F, Sulpice A and Caneschi A 1998 *J. Magn. Magn. Mater.* **177–181** 1324
[30] Barbara B, Thomas L, Lionti F, Chiorescu I and Sulpice A 1999 *J. Magn. Magn. Mater.* **200** 167
[31] Wernsdorfer W, Ohm T, Sangregorio C, Sessoli R, Mailly D and Paulsen C 1999 *Phys. Rev. Lett.* **82** 3903
[32] Jang Z H, Lascialfari A, Borsa F and Gatteschi D 2000 *Phys. Rev. Lett.* **84** 2977
[33] Gatteschi D and Sessoli R 2003 *Angewandte Chemie International Edition* **42** 268
[34] Leuenberger M N and Loss D 2000 *Phys. Rev. B* **61** 1286
[35] Kent A D, Zhong Y, Bokacheva L, Ruiz D, Hendrickson D N and Sarachik M P 2000 *J. Appl. Phys.* **87** 5493
[36] Kent A D, Zhong Y, Bokacheva L, Ruiz D, Hendrickson D N and Sarachik M P 2000 *Europhys. Lett.* **49** 521
[37] Zhong Y, Sarachik M P, Yoo J and Hendrickson D N 2000 *Phys. Rev. B* **62** R9256
[38] Chiorescu I, Giraud R, Jansen A G M, Caneschi A and Barbara B 2000 *Phys. Rev. Lett.* **85** 4807
[39] Fort A, Rettori A, Villain J, Gatteschi D and Sessoli R 1998 *Phys. Rev. Lett.* **80** 612
[40] Garanin D A and Chudnovsky E M 1997 *Phys. Rev. B* **56** 11102
[41] Luis F, Bartolomé J and Fernández J F 1998 *Phys. Rev. B* **57** 505
[42] Harman W H, Harris T D, Freedman D E, Fong H, Chang A, Rinehart J D, Ozarowski A, Sougrati M T, Grandjean F, Long G J, Long J R and Chang C J 2010 *J. Am. Chem. Soc.* **132** 18115
[43] Vallejo J, Castro I, Ruiz-García R, Cano J, Julve M, Lloret F, Munno G D, Wernsdorfer W and Pardo E 2012 *J. Am. Chem. Soc.* **134** 15704
[44] Zhu Y Y, Cui C, Zhang Y Q, Jia J H, Guo X, Gao C, Qian K, Jiang S D, Wang B W, Wang Z M and Gao S 2013 *Chem. Sci.* **4** 1802
[45] Zadrozny J M, Atanasov M, Bryan A M, Lin C Y, Rekken B D, Power P P, Neese F and Long J R 2013 *Chem. Sci.* **4** 125
[46] Lucaccini E, Sorace L, Perfetti M, Costes J P and Sessoli R 2014 *Chem. Commun.* **50** 1648
[47] Gómez-Coca S, Urtizberea A, Cremades E, Alonso P J, Camón A, Ruiz E and Luis F 2014 *Nat. Commun.* **5** 4300
[48] Liddle S T and van Slageren J 2015 *Chem. Soc. Rev.* **44** 6655
[49] Rajnák C, Titiš J, Moncoľ J, Renz F and Boča R 2019 *Chem. Commun.* **55** 13868
[50] Wang J, Ruan Z Y, Li Q W, Chen Y C, Huang G Z, Liu J L, Reta D, Chilton N F, Wang Z X and Tong M L 2019 *Dalton Transactions* **48** 1686
[51] Kobayashi F, Ohtani R, Nakamura M, Lindoy L F and Hayami S 2019 *Inorganic Chemistry* **58** 7409
[52] Cui H H, Lu F, Chen X T, Zhang Y Q, Tong W and Xue Z L 2019 *Inorganic Chemistry* **58** 12555
[53] Wäckerlin C, Donati F, Singha A, Baltic R, Rusponi S, Diller K, Patthey F, Pivetta M, Lan Y, Klyatskaya S, Ruben M, Brune H and Dreiser J 2016 *Adv. Mater.* **28** 5195
[54] Goodwin C A P, Ortu F, Reta D, Chilton N F and Mills D P 2017 *Nature* **548** 439
[55] Abbasi P, Quinn K, Alexandropoulos D I, Damjanović M, Wernsdorfer W, Escuer A, Mayans J, Pilkington M and Stamatatos T C 2017 *J. Am. Chem. Soc.* **139** 15644
[56] Guo F S, Day B M, Chen Y C, Tong M L, Mansikkamäki A and Layfield R A 2018 *Science* **362** 1400
[57] Randall McClain K, Gould C A, Chakarawet K, Teat S J, Groshens T J, Long J R and Harvey B G 2018 *Chem. Sci.* **9** 8492
[58] Gould C A, McClain K R, Reta D, Kragskow J G C, Marchiori D A, Lachman E, Choi E S, Analytis J G, Britt R D, Chilton N F, Harvey B G and Long J R 2022 *Science* **375** 198
[59] Kragskow J G C, Mattioni A, Staab J K, Reta D, Skelton J M and Chilton N F 2023 *Chem. Soc. Rev.* **52** 4567
[60] Breuer H P and Petruccione F 2002 *The theory of open quantum systems* (Oxford: Oxford University Press)
[61] Calero C, Chudnovsky E M and Garanin D A 2006 *Phys. Rev. B* **74** 094428
[62] Ho L T A and Chibotaru L F 2018 *Phys. Rev. B* **97** 024427
[63] Chiesa A, Cugini F, Hussain R, Macaluso E, Allodi G, Garlatti E, Giansiracusa M, Goodwin C A P, Ortu F, Reta D, Skelton J M, Guidi T, Santini P, Solzi M, De Renzi R, Mills D P, Chilton N F and Carretta S 2020 *Phys. Rev. B* **101** 174402
[64] Nabi R, Staab J K, Mattioni A, Kragskow J G C, Reta D, Skelton J M and Chilton N F 2023 *J. Am. Chem. Soc.* **145** 24558
[65] Abragam A and Bleaney B 2012 *Electron paramagnetic resonance of transition ions* (Oxford: Oxford University Press)